31st Annual International Conference of the IEEE EMBS
Minneapolis, Minnesota, USA, September 2-6, 2009

Extended Time-frequency Granger Causality for Evaluation of Functional Network Connectivity in Event-related FMRI Data

M. Havlicek, J. Jan, V.D. Calhoun, *Senior Member, IEEE,* and M. Brazdil

Abstract— **In this article, we show that adaptive multivariate autoregressive (AMVAR) modeling accompanied by proper estimation of the delay and the width of hemodynamic response function is an effective technique for evaluation of spectral Granger causality among different functional brain networks identified by independent component analysis from event-related fMRI data. The entire concept is demonstrated on 28 subjects auditory oddball fMRI data.**

I. Introduction

THE concept of functional connectivity in the analysis of functional MRI data, which is defined as the correlations between spatially remote neurophysiological events [1], was recently extended to the concept of functional network connectivity (FNC) [2]. The goal of FNC is to characterize distributed changes in the brain by examining the functional interaction among different correlated brain networks, usually identified by independent component analysis (ICA).

There have been several attempts to investigate the directional influence among different activated brain regions by using a Granger causality test [3] in either the time [4] or the spectral [5] domain. However, in both cases the basic assumption of stationarity required by Granger's method was utilized. This is a concern as the fMRI time courses are known to be highly nonstationary [6].

Therefore, we proposed a method which can work better with nonstationary data based on parametric spectral analysis in which multivariate autoregressive (MVAR) time series models are adaptively extracted from the data using short windows and become the basis for deriving spectral quantities. Previously, we applied and validated this method via simulation of event-related fMRI data [7]. The latency and shape of hemodynamic response to stimulus vary among different brain regions within one subject as well as cross subjects. In order to take this variance into account, we introduce an extension of the MVAR model based on the estimation of hemodynamic response parameters.

In this paper we evaluate the capability of our approach on real event-related fMRI data.

The main concept of our approach arises from the causality expectation, i.e. that if the stimulation event occurs, then the response will follow. Therefore, we can consider only these parts of the signal that appear in the estimated window subsequent to the stimulus.

We propose the following procedure for a time-frequency based evaluation of FNC during a cognitive task:

1) Perform fMRI data analysis by ICA and select unique time courses of components of interest.
2) Do necessary preprocessing for each time course.
3) Estimate the delay and the width of the main lobe of hemodynamic response function (HRF).
4) Split each time course into equal segments that take into account the HRF width, so that their origins are based on the event onset function and the estimated HRF delay.
5) For each window apply MVAR model by fitting data from a set of segments.
6) Derive the transfer function and the spectral matrix from the model coefficients.
7) Use these spectral quantities to calculate causal influence between pairs of time courses and identify the frequency profiles at a window position with the highest value of Granger Causality.

II. Methods

A. Independent Component Analysis

ICA is a multivariate statistical technique that uses higher order statistic to separate observed signals into maximally independent components.

For fMRI data, the typical approach is to identify maximally spatially independent components (sICA), i.e. spatially independent brain networks, each with its associated time course. In this case, the raw data are considered to be linear mixture of spatial activated maps, assumed to be maximally independent while their corresponding time courses are unconstrained [8].

Manuscript received April 7, 2009. This work has been sponsored by the research center DAR no. 1M0572, and also supported by the research frame no. MSM0021630513 and no. MSM0021622404, all funded by the Ministry of Education, Czech Republic. From the USA side, it has been generously funded by NIH grant no. R01 EB000840.

M. Havlicek is with the Department of Biomedical Engineering, University of Technology Brno, Czech Republic, and with the Mind Research Network, Albuquerque, NM, USA (e-mail: havlicekm@phd.feec.vutbr.cz).

J. Jan is with the Department of Biomedical Engineering, University of Technology Brno, Czech Republic (email: jan@feec.vutbr.cz).

V. D. Calhoun is with the Mind Research Network and the Department of ECE, University of New Mexico, Albuquerque, NM, USA (e-mail: vcalhoun@unm.edu).

M. Brazdil is with the Department of Neurology, St. Anne's University Hospital, and Faculty of Medicine, Masaryk University, Brno, Czech Republic (e-mail: mbrazd@med.muni.cz).

B. Estimation of HRF Parameters

HRF delay: is estimated using general linear model (GLM), where we consider theoretical HRF approximated as a difference of two gamma functions with 6 s peak latency, convolved with the stimulus onset function. We propose seeking the delay by shifting the origin of the HRF by δ in the range ($-4.5 \le \delta \ge 4.5$) s. The HRF delay (d) is then identified as the best fit of the linear model

$$Y = \mathbf{X}(t-\delta)\beta_\delta + \varepsilon_\delta, \tag{1}$$

where Y is the independent component (IC) time course, $\mathbf{X}$ is design matrix, which contains modeled time course and low-frequency cosine transform basis functions for removing signal drift. β_δ and ε_δ are the model coefficient estimated in the least square sense for particular HRF delay δ, and the model error, respectively.

HRF width: is estimated applying simple deconvolution of event-related HRF by forming the convolution matrix of the stimulus onset function with assumed kernel length 22 s, and multiplying the pseudoinverse of this matrix with IC time course. Final HRF width (w) is calculated as the distance between two nearest minimums around the main HRF lobe, see Fig. 2.

C. Estimation of MVAR Model

Let $\mathbf{Y}(t)=[Y_1(t),Y_2(t),\ldots Y_p(t)]^{\mathrm{T}}$ be a p-dimensional random process defined in a segment of windowed time series data, where T denotes matrix transposition. In our case, p represents the total number of time series of independent components. Assuming stationarity of the process $\mathbf{Y}(t)$ in each window, one can describe $\mathbf{Y}(t)$ in each window by pth-order autoregressive equation

$$\mathbf{E}(t) = \mathbf{Y}(t) + \mathbf{A}(1)\mathbf{Y}(t-1) + \ldots + \mathbf{A}(m)\mathbf{Y}(t-m), \tag{2}$$

where $\mathbf{A}(i)$ are $p \times p$ matrices and $\mathbf{E}(t)$ is a p-dimensional, zero mean, uncorrelated noise vector with covariance matrix $\mathbf{\Sigma}$. In order to estimate $\mathbf{A}(i)$ and $\mathbf{\Sigma}$ we can apply the Levinson, Wiggings, Robinson (LWR) algorithm [9], which is based on the ideas of maximum entropy.

The estimation should be performed for correct model order m that can be determined by minimizing Bayesian Information Criterion (BIC) defined as

$$\mathbf{BIC} = 2\log[\det(\mathbf{\Sigma})] + \frac{2p^2 m \log N_{total}}{N_{total}}, \tag{3}$$

where N_{total} is total number of data points from entire segment. It should be noted that we estimate the model order for each single segment and then the average order is used in AMVAR model.

D. Spectral Granger Causality

Whenever the model coefficient matrix $\mathbf{A}(i)$ and the covariance matrix $\mathbf{\Sigma}$ of the noise are estimated, the spectral quantities can be derived in the frequency domain. From the transfer function

$$\mathbf{H}(f) = \left(\sum_{i=0}^{m} \mathbf{A}(i) e^{-ji2\pi f} \right)^{-1}, \tag{4}$$

the spectral matrix of the time series is given by

$$\mathbf{S}(f) = \mathbf{H}(f)\mathbf{\Sigma}\mathbf{H}^{*}(f), \tag{5}$$

from which the Granger causality can be derived. According to Geweke's formulation [10], the Granger causal influence from time series i to time series j is given by

$$F_{i\to j}(f) = -\log\left(1 - (\Sigma_{j,j} - \frac{\Sigma_{i,j}^2}{\Sigma_{j,j}}) \frac{|H_{i,j}(f)|^2}{S_{i,i}(f)}\right), \tag{6}$$

It is evident that if $F_{i\to j} = 0$, then there is no causal influence from i to j and if $F_{i\to j} > 0$, then the influence exists, and vice versa. Equation (6) enables us to measure causality only between two components, but because we are able to estimate autoregressive models for arbitrary number of time series, we can identify also the direct or indirect influences from other components.

III. FMRI DATA

Functional data of 28 healthy volunteers, who were scanned during an auditory oddball task (AOD), were used.

Experimental design: The AOD consists of detecting an infrequent sound within a series of regular and different sounds (standard stimulus – 500 Hz tone, target stimulus 1000 Hz, and novel stimuli – nonrepeating random digital noise, e.g. tone sweeps, whistles). The stimulus duration was 200 ms and participants were instructed to respond with their right index finger every time they heard the target stimulus and not to respond to the nontarget or novel stimuli.

Image Acquisition: Scans were acquired at the Olin Neuropsychiatry Research Center at the Institute of Living/Hartford Hospital on a Siemens Allegra 3T MRI scanner. The functional scans were acquired transaxially using gradient-echo echo-planar-imaging with the following parameters (repeat time (TR) = 1.5 s, echo time (TE) = 27 ms, field of view 24 cm, acquisition matrix = 64 × 64, flip angle = 70º, voxel size = 3.75 × 3.75 × 4 mm^3, slice thickness = 4 mm, gap = 1 mm, 29 slices in ascending order).

Preprocessing: Data were preprocessed using SPM5 software (http://fil.ion.ucl.ac.uk/spm/software/spm5/). Data were motion corrected, spatially normalized into standard MNI space and slightly subsampled to voxel size 3 × 3 × 3 mm^3, resulting in 53 × 63 × 46 voxels. Next, the spatial

smoothing with 10 × 10 × 10 mm^3 FWHM Gaussian kernel was performed. Group spatial ICA [10] was used to decompose all data into components using GIFT software (http://icatb.sourceforge.net/). The number of components was estimated to be 19 [12]. Data from all subjects were concatenated and this aggregate data set then reduced to 19 temporal dimensions using PCA, followed by independent component estimation using infomax algorithm [13].

Component selection: IC spatial maps were then reconstructed and converted to Z score values. The time courses of the components were regressed with the designs used in the tasks and independent components were sorted according to their importance. After visual inspection of sorted spatial maps, four components and their associated time courses were selected: anterior cingulate (TC1), posterior cingulate-precuneus (TC8), primary auditory areas (TC16), prefrontal cortex (TC18).

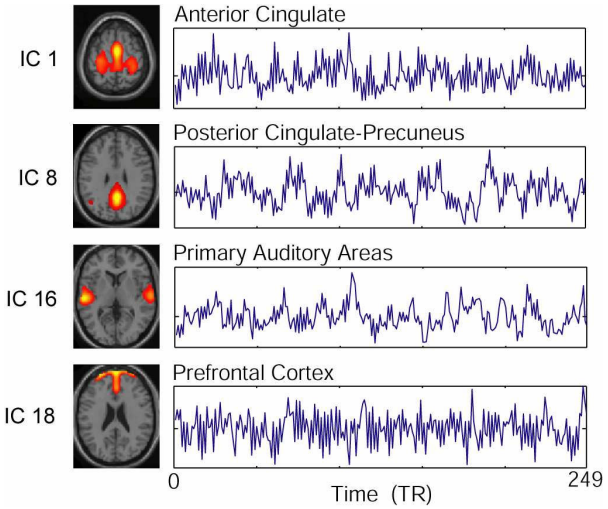

Fig. 1. Selected spatial maps of independent components and their associated time courses. Spatial maps are threshold at $p < 0.01$.

IV. Results

After applying ICA to fMRI data and selecting component time courses among which we want to test causal influence, several following preprocessing steps were performed: low-pass filtering with cut-off normalized frequency 0.2; high-pass filtering based on discrete cosine transform functions to remove very low frequencies, i.e. signal drift; zero-mean correction and standard deviation normalization; and resampling by factor 10. For interpolation we used a cubic method.

A. Time-courses Segmentation

The latency of HRF on stimulus and also HRF duration can be very varying within one subject in different activated brain areas. This is what we are looking for in order to examine their dynamic interactions but it can be also variable across multiple subjects, even for the same brain region. To handle this, we have adaptively estimated the HRF delay and duration for each single component time course and used their minimal and average values, respectively, for adjusting starting points and the width of shifting window within each single subject. Then the total length of the segment, including the interval for window shift, was considered as (w + w/3). The exact starting position of segments was calculated as (onset timing + estimated minimal HRF delay – 2 s). Here, we have subtracted 2 s in order to include even the already ascending part of HRF main lobe. In this case, we were interested in the effect of targets stimuli.

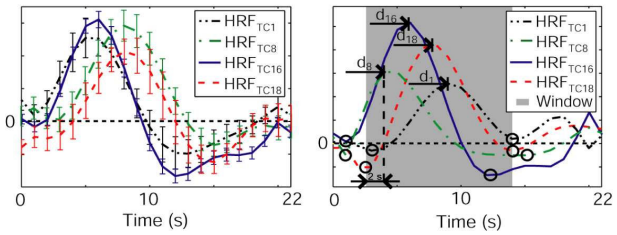

Fig. 2. Deconvolved HRFs averaged over all subjects with the standard error measurement (on the left). Illustration of estimated HRF delays and selection of window width according to found minima around the main HRF lobe (on the right).

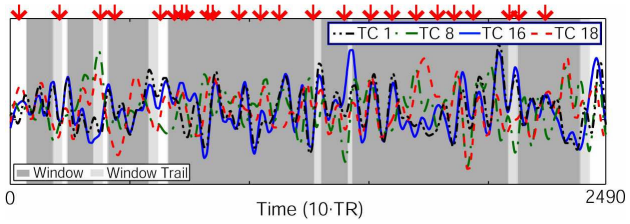

Fig. 3. Interpolated time courses with illustration of considered short time windows and their trails, including stimulus onset of targets (arrows). The high segments overlap can be seen.

B. MVAR Modeling and Granger Causality

Once we partition time courses into sets of segments, we again perform mean removal and normalization by standard deviation on each segment. The model order was estimated for each segment based on BIC as well and the average value was applied in MVAR model. Then the coefficients of MVAR and spectral quantities were estimated for each window position inside segments. Since the causal influence (6) was calculated for each window position, finally we obtained a spectrogram of the Granger causality (Fig. 4, on the left), where dynamic changes of causal influence between two time courses during short window movement can be seen. By selecting the frequency profile with the maximal amplitude from the spectrograms, related to both tested causal directions and by their subsequent comparison, we identified the prevalent causal direction and also main driving frequency (Fig. 4, on the right).

Our approach identified very significant directional influence from primary auditory areas (TC16) and posterior cingulate-precuneus (TC8) to prefrontal cortex (TC18). The causality from anterior cingulate (TC1) to prefrontal cortex

(TC18) is dominant as well. The other connections have also distinctly increased nonzero values of Granger causality, however no significantly prevalent direction was proved. Therefore, these connections are considered as bidirectional.

The results represent the average over all 28 subjects, when we used both data sessions together. It is worth to note that although we estimated MVAR model for each session separately, we have obtained the same connectivity configuration. This apparently supports our hypothesis that the introduced model is correct.

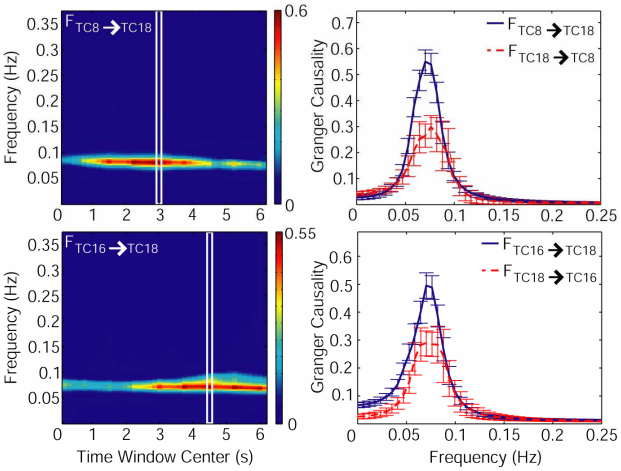

Fig. 4. The example of spectrograms of Granger causality among component time courses (on the left), and individual spectra of maximal Granger causality for two most significant connections (TC16 → TC18 and TC8 → TC18). Spectra represent the average over all subjects with depiction of measurement standard error (on the right).

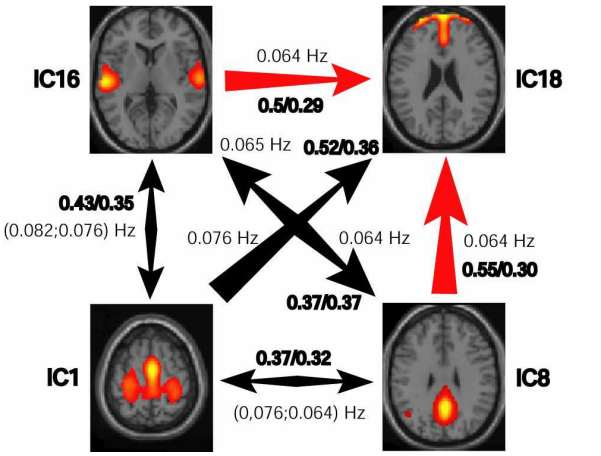

Fig. 5. Estimated integration of the functional network connectivity with indicated values of Granger causality (prevalent direction/nonprevalent direction) and driving frequencies.

V. Conclusion

We introduced the concept of the identification of causal influence among functional brain networks in the event-related fMRI data by combining the ICA and a spectral Granger test via AMVAR time series modeling over short overlapping time windows of the time courses.

We have applied our method to the real event-related fMRI data (AOD). In contrast to the previous version [7], we have extended our model by proper estimation of the HRF delay and HRF width from the independent component time courses. This procedure notably improves the estimation of MVAR model.

Compared to the ordinary Granger's model, which a priori assumes stationarity of data, not completely valid in the case of fMRI data, our approach handles more generic nonstationary data by performing MVAR analysis in short, highly overlapped windows, in which stochastic processes are considered to be locally stationary. By adaptively estimating MVAR model in each window, we exploit the time-frequency representation of time series to manifest causal relationship in different frequency bands, as well as at different time instants.

Finally, our approach also enables one to examine FNC integration under different experimental events and it might become an effective tool in resolving and evaluating functional brain network connectivity.

References

[1] K. Friston, "Functional and effective connectivity in neuroimaging: a synthesis," *Hum Brain Mapp*, vol. 2, 1994.

[2] M. Jafri, G. Pearlson, M. Stevens, and V. Calhoun, "A method for functional network connectivity among spatially independent resting-state components in schizophrenia," *Neuroimage*, vol. 39, pp. 1666-1681, 2008.

[3] C. Granger, "Investigating causal relations by econometric models and cross-spectral methods," *Econometrica*, pp. 424-438, 1969.

[4] A. Londei, A. D'Ausilio, D. Basso, and M. Belardinelli, "A new method for detecting causality in fMRI data of cognitive processing," *Cogn Process*, vol. 7, pp. 42-52, 2006.

[5] O. Demirci, M. Stevens, N. Andreasen, A. Michael, J. Liu, et al., "Investigation of relationships between fMRI brain networks in the spectral domain using ICA and Granger causality reveals distinct differences between schizophrenia patients and healthy controls," *Neuroimage*, vol. 46, (no. 2), pp. 419-431, 2009.

[6] B. Gaschler-Markefski, F. Baumgart, C. Tempelmann, F. Schindler, et al., "Statistical methods in functional magnetic resonance imaging with respect to nonstationary time series: Auditory cortex activity," *Mag Res in Med*, vol. 38, pp. 811-820, 1997.

[7] M. Havlicek, J. Jan, V.D. Calhoun, M. Brazdil, "Evaluation of Functional network connectivity in event-related fMRI data based on ICA and time-frequency Granger Causality," *IFMBE Conference*, 2009, accepted publication.

[8] M. McKeown, S. Makeig, G. Brown, T. Jung, S. Kindermann, A. Bell, and T. Sejnowski, "Analysis of fMRI data by blind separation into independent spatial components," *Hum Brain Mapp*, vol. 6, 1998.

[9] M. Morf, A. Vieira, D. Lee, and T. Kailath, "Recursive multichannel maximum entropy spectral estimation," *IEEE Trans on Geosci Electron*, vol. 16, (no. 2), pp. 85-94, 1978.

[10] J. Geweke, "Measurement of linear dependence and feedback between multiple time series," *J Am Stat Assoc*, pp. 304-313, 1982.

[11] V. Calhoun, T. Adali, G. Pearlson, and J. Pekar, "A method for making group inferences from functional MRI data using independent component analysis," *Hum Brain Mapp*, vol. 16, pp. 131-131, 2002.

[12] Y. Li, T. Adali, and V. Calhoun, "Estimating the number of independent components for functional magnetic resonance imaging data," *Hum Brain Mapp*, vol. 28, 2007.

[13] A. Bell and T. Sejnowski, "An information-maximization approach to blind separation and blind deconvolution," *Neural Comput*, vol. 7, pp. 1129-1159, 1995.